Transworld Research Network
37/661 (2), Fort P.O., Trivandrum-695 023, Kerala, India

New Developments in Quantum Chemistry, 2009: 25-54 ISBN: 978-81-7895-446-2
Editors: José Luis Paz and Antonio J. Hernández

2 Recent advances in developing orbital-free kinetic energy functionals

V.V. Karasiev[1], R.S. Jones[2], S.B. Trickey[3] and Frank E. Harris[4]
[1]Centro de Química, Instituto Venezolano de Investigaciones Científicas IVIC, Apartado 21827, Caracas 1020-A, Venezuela and Quantum Theory Project, Departments of Physics and of Chemistry, University of Florida Gainesville, FL 32611, USA; [2]Dept. of Physics, Loyola College in Maryland 4501 N. Charles Street, Baltimore, MD 21210; [3]Quantum Theory Project Dept. of Physics and Dept. of Chemistry, University of Florida, Gainesville FL 32611, USA; [4]Dept. of Physics, University of Utah, Salt Lake City, UT and Quantum Theory Project, Dept. of Chemistry, University of Florida Gainesville, FL 32611, USA

I. Introduction

Density functional theory (DFT) [1–3] is the standard tool of modern computational materials physics and much of quantum chemistry. The present-day range of materials science, nano-scale, and bio-molecular applications of DFT is vastly wider than that of wave-function-based methods

Correspondence/Reprint request: Dr. V.V. Karasiev, Centro de Química, Instituto Venezolano de Investigaciones Científicas, IVIC, Apartado 21827, Caracas 1020-A, Venezuela and Quantum Theory Project, Departments of Physics and of Chemistry, University of Florida, Gainesville, FL 32611, USA
E-mail: vkarasev@qtp.uf1.edu

because DFT methods are faster (require less computational resources) especially for relatively large systems (~ 1000 atoms). Only at high order and great computational expense do wave-function-based methods (so-called "*ab initio*" methods) routinely excel in accuracy relative to DFT.

To establish notation and terminology, we summarize the conventional Kohn-Sham (KS) approach [4] in non-spin-polarized form. To use the variational principle in DFT, Kohn and Sham introduced a reference (or "fictitious", a somewhat misleading term) system of N_e non-interacting fermions with the same electron density $n = n_\Psi$ as the real many-electron system in its ground state $|\Psi\rangle$. These independent particles move in the effective potential v_{KS}. The total energy then is decomposed into an explicit functional of individual one-particle orbitals, $\{\phi_i\}_{i=1}^{N_e/2}$, and several explicit functionals of the electron density:

$$E^{\mathrm{KS\text{-}DFT}}[\{\phi_i\}_{i=1}^{N'}, n] = T_s[\{\phi_i\}_{i=1}^{N'}] + E_{\mathrm{ne}}[n] + E_{\mathrm{H}}[n] + E_{\mathrm{xc}}[n] + E_{\mathrm{ion}}\,. \quad (1)$$

Here $N' \equiv N_e/2$. $E_{\mathrm{ne}}[n]$, $E_{\mathrm{H}}[n]$, $E_{\mathrm{xc}}[n]$ are respectively the usual nuclear-electron attraction, Hartree (or classical Coulomb) electron repulsion, and electron exchange-correlation energy functionals, and E_{ion} is the energy of nuclear-nuclear repulsion (or that of ion-ion repulsion in the case of pseudopotentials). The orbitals are implicitly functionals of the electron density, n, through the requirement

$$n(\mathbf{r}) = 2\sum_{i}^{N'} \phi_i^*(\mathbf{r})\,\phi_i(\mathbf{r})\,. \quad (2)$$

The explicitly orbital-dependent term T_s on the RHS of Eq. (1) is the kinetic energy (KE) of the model non-interacting system:

$$\begin{aligned} T_s[\{\phi_i\}_{i=1}^{N'}] &= 2\sum_{i=1}^{N_e/2} \int \phi_i^*(\mathbf{r})(-\frac{1}{2}\nabla^2)\phi_i(\mathbf{r})d^3\mathbf{r} \\ &\equiv \int t_{\mathrm{orb}}(\mathbf{r})d^3\mathbf{r}\,. \end{aligned} \quad (3)$$

(We use Hartree atomic units unless indicated otherwise.) The difference between the interacting system KE and the KS model (non-interacting) system KE, $\langle\Psi|\hat{T}|\Psi\rangle - T_s$, is a part of the DFT exchange-correlation functional $E_{\mathrm{xc}}[n]$. Variational minimization leads to a system of differential equations for the KS orbitals $\{\phi_i\}_{i=1}^{N'}$:

$$\left\{-\frac{1}{2}\nabla^2 + v_{\mathrm{KS}}([n];\mathbf{r})\right\}\phi_i(\mathbf{r}) = \varepsilon_i\phi_i(\mathbf{r})\ . \tag{4}$$

The effective potential v_{KS} is the functional derivative with respect to density of the sum of the explicitly *n*-dependent terms on the RHS of Eq. (1):

$$v_{\mathrm{KS}}([n];\mathbf{r}) \equiv \frac{\delta}{\delta n(\mathbf{r})}\Big(E_{\mathrm{ne}}[n] + E_{\mathrm{H}}[n] + E_{\mathrm{xc}}[n]\Big)\ . \tag{5}$$

The main computational disadvantage of the KS approach is the explicit use of one-particle orbitals (though that also is part of the ingenuity of the method). Their presence is a serious barrier to repeated applications on large (> 1000 atoms) systems because of the scaling of computational cost with particle number. At least formally the scaling is $O(N^3)$, where N is proportional to N_e. Even with so-called order-N approximations (which are not general), the KS approach has this limitation. A major objective therefore is scaling with system volume (unit cell, simulation cell, etc.) rather than system population.

One of the applications which illustrates the criticality of this objective is calculation of Born-Oppenheimer (B-O) forces for driving the so-called quantum region of multi-scale molecular dynamics (MD) simulations. In such simulations, the system is partitioned into two types of zones. One is the chemically active, so-called quantum zone which typically is far from equilibrium and in which bond-breaking may occur. The other is an enclosing zone in which the internuclear forces are calculated from a classical potential. Because MD may require 10^3 to 10^5 or more steps, evaluation of forces in the quantum zone requires a fast quantum mechanical method that does not sacrifice realism.

An alternative approach to the use of KS orbitals is orbital-free (OF) DFT. In it, the total energy is expressed as a pure, explicit density functional

$$E^{\text{OF-DFT}}[n] = T_s[n] + E_{\mathrm{ne}}[n] + E_{\mathrm{H}}[n] + E_{\mathrm{xc}}[n] + E_{\mathrm{ion}}\ . \tag{6}$$

Then, instead of a self-consistent field problem for N' KS orbitals, the variational minimization yields a single Euler equation:

$$\frac{\delta T_s[n]}{\delta n(\mathbf{r})} + v_{\mathrm{KS}}([n];\mathbf{r}) = \mu\ . \tag{7}$$

Here μ is the Lagrange multiplier associated with density normalization, $\int n(\mathbf{r})d^3\mathbf{r} = N_e$. Thus, in principle, the computational cost of OF-DFT

methods does not depend on the number of particles in the system since only a single equation, Eq. (7), need be solved irrespective of N_e. The computational cost therefore should scale as the spatial extent of the system.

The main barrier to widespread use of OF-DFT has been finding reliable approximations for the KS kinetic energy T_s as an explicit functional of the density. Note that the focus on T_s is important both conceptually and practically. The conceptual point is that the Coulomb virial theorem suggests very strongly that an effort to find the full T [n] would be tantamount to trying to find the universal functional whose existence was demonstrated by Hohenberg and Kohn [5]. The practical issue is that successful approximate $E_{\rm xc}$ functionals were developed in the context of T_s.

The challenge of finding good KE functionals dates to the formulation of the primordial DFT, namely the Thomas-Fermi (TF) model [6, 7]. For the homogeneous electron gas, the TF noninteracting KE functional is

$$T_{\rm TF}[n] \equiv \int t_{\rm TF}[n(\mathbf{r})]\, d^3\mathbf{r} = c_0 \int n^{5/3}(\mathbf{r})\, d^3\mathbf{r}, \tag{8}$$

where $c_0 = \frac{3}{10}(3\pi^2)^{2/3}$. Solution of Eq. (7) with the TF model is inexpensive, but useless for real systems. The TF functional does not yield even a qualitatively correct representation of bound systems. Indeed, it cannot, as demonstrated by Teller's non-bonding theorem [8]. Despite this fundamental flaw, one still encounters the TF functional in OF-DFT calculations (see Refs. [9–12]).

Another simple KE functional is the von Weizsäcker form

$$T_{\rm W}[n] = \int \frac{1}{8}\frac{|\nabla n(\mathbf{r})|^2}{n(\mathbf{r})}\, d^3\mathbf{r} \equiv \int t_{\rm W}([n];\mathbf{r})\, d^3\mathbf{r}\,. \tag{9}$$

It is exact for one-electron and two-electron singlet states [13]. A linear combination of these two simplest approximations, TF and von Weizsäcker, has seen wide use in many OF-DFT applications (see discussion and references in Ref. [14]).

Generally, explicit KE energy functionals may be presented as expansions depending on the density and its higher-order spatial derivatives in the following "semi-local" form (for examples, see Refs. [15–24]):

$$T_s[n] = \int t_s(n(\mathbf{r}), |\nabla n(\mathbf{r})|, \nabla^2 n(\mathbf{r}), ...)\, d^3\mathbf{r}\,. \tag{10}$$

Strictly, these are local functionals; "semi-local" refers loosely to the estimate of non-local behavior from derivatives.

An alternative approach, which has drawn substantial attention in recent years, involves the introduction of two-point or non-local functionals of the form

$$T_s^{\text{nonloc}}[n] = \int\int n(\mathbf{r})\, w(\mathbf{r},\mathbf{r}')\, n(\mathbf{r}')\, d^3\mathbf{r}\, d^3\mathbf{r}' , \tag{11}$$

Note that the two-point function w also may depend on the density [9–11]. The challenge for such two-point functionals again is two-fold: computational speed and compatibility with successful one-point exchange-correlation (XC) functionals.

An approximate OF-DFT functional intended to provide B-O forces for MD must be correct not only at equilibrium nuclear geometries but also for states far from equilibrium. The purpose of the present work is to discuss recent advances in developing simple one-point kinetic energy functionals capable of predicting correctly the B-O interatomic forces for such MD applications of OF-DFT. In Section II, we start with a brief review of explicit one-point KE functionals that have been proposed previously by others. These functionals are based on the gradient expansion approximation (GEA) and the generalized gradient approximation (GGA), and in some cases also are motivated by the notion of "conjointness" [25]. In Subsections A and B we describe tests that show the failure of these functionals to predict, even qualitatively, the interatomic forces in the attractive region (near equilibrium) of simple molecules. In Subsections C and D we introduce some essential background and examine the extent to which existing functionals satisfy important constraints on the behavior of OF-KE approximations. Then, in Subsection E we describe the "modified conjoint" functionals we have developed for qualitatively or even semi-quantitatively correct prediction of B-O forces. Section III introduces new approximations for OF-KE functionals which arise from application of new constraints developed to eliminate near-nucleus singularities. That Section also includes exploratory tests of simultaneous prediction of the absolute value of the total energy and B-O forces. In Section IV we summarize the results of some severe tests of our OF-DFT approximations on solids. We close with Section V, a short Discussion.

Please note that, for convenience, in the present work we deal with functionals of the total density only, $T_s[n]$. Spin-polarized (open shell) systems could be treated with the appropriate spin-density generalization [26], to wit:

$$T_s[n_\uparrow, n_\downarrow] = \frac{1}{2}T_s[2n_\uparrow] + \frac{1}{2}T_s[2n_\downarrow] . \tag{12}$$

II. Explicit kinetic energy density functionals

A. Kinetic and total energy

First we illustrate the present situation distinct from our own work. Many KE functionals have been presented in the literature with supporting arguments for claims of accuracy and utility. As an initial test of such claims, we selected six representative published KE functionals and studied their performance on a collection of diatomic and small polyatomic molecules in their equilibrium geometries. We began by determining the geometries and electron densities produced by conventional KS calculations in the local density approximation (LDA, a standard combination of the Slater exchange functional [27] and the Vosko, Wilk, and Nusair (VWN) approximation for correlation [28]). Then, for those geometries and densities, we compared, see Table I, the KS kinetic energies T_s with those predicted by the various KE functionals. Table I includes the Thomas-Fermi (TF) and von Weizsäcker (W) functionals, the second-order gradient expansion approximation (SGA), a GGA functional proposed by Perdew (GGA-P), the "PW91" functional of Lacks and Gordon, and the empirical or semi-empirical functionals of DePristo and Kress (DPK), Thakkar, and Tran and Wesolowski (PBE-TW). The details of the latter six (newer) functionals are presented in Section II-D. What is relevant here is the outcome of the test itself. Notice that the design objective of the KE functionals examined here was that they reproduce the KS kinetic energy as calculated by Eq. (3), which is therefore the correct answer in this context. We see that the TF and W functionals yield significant underestimates for all molecules except the two-electron case (the H_2 molecule), for which the von Weizsäcker functional is exact. As the number of electrons increases, however, the W functional rapidly becomes poorer than TF. The newer KE functionals have significantly smaller percentage

Table I. KS kinetic energy T_s values (in Hartrees) for selected molecules calculated using a representative set of explicit semi-local approximate functionals (see Sec. II-D for definitions). LDA-KS densities for LDA equilibrium geometries (with TZVP basis set) were used as input.

	TF	W	SGA	GGA-P	PW91	DPK	Thakkar	PBE-TW	KS
H_2	0.946	1.080	1.066	1.066	1.052	1.062	1.059	1.053	1.080
LiH	6.961	7.499	7.794	7.796	7.760	7.705	7.804	7.769	7.784
H_2O	68.526	56.794	74.837	74.849	75.143	74.830	75.217	75.171	75.502
FH	90.494	72.160	98.512	98.528	99.000	98.705	99.037	99.018	99.390
N_2	97.764	84.986	107.207	107.225	107.531	106.867	107.723	107.599	108.062
CO	101.296	86.928	110.955	110.974	111.325	110.683	111.498	111.385	111.832
NaF	238.158	181.927	258.372	258.412	259.827	259.205	259.750	259.824	260.097
F_2O	246.574	200.207	268.819	268.863	270.077	269.039	270.257	270.150	271.733
SiO	333.840	238.457	360.335	360.387	362.662	361.848	362.180	362.553	362.442
H_4SiO	336.040	239.661	362.669	362.721	365.002	364.194	364.509	364.890	364.672

errors than the TF and W forms, either because they incorporate more density gradient information (SGA, GGA-P, PW91) or because they were fitted to give correct results for training sets of atoms (DPK, PBE-TW) or molecules (Thakkar). One might be tempted to conclude from Table I that the newer KE functionals are qualitatively satisfactory.

However, as a second and more crucial test, the same six approximate functionals were used for calculation of the KS kinetic energy and corresponding total energy for deformed geometries of simple molecules. The left-hand panels of Figs. 1 and 2 show the total energy as a function of

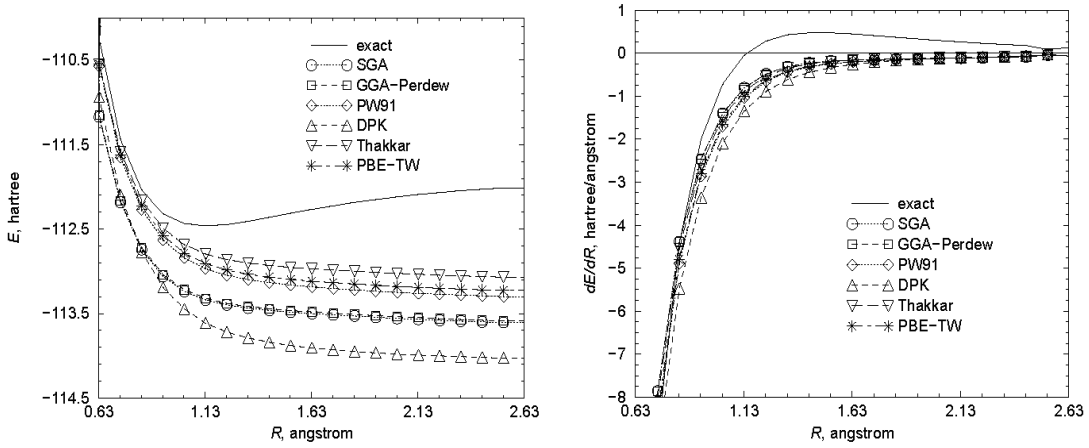

Figure 1. Total energy (left panel) and gradient of the total energy (right panel) of the CO molecule as a function of bond length, calculated using six approximate OF-KE functionals, with the KS-LDA densities (TZVP basis set) as input.

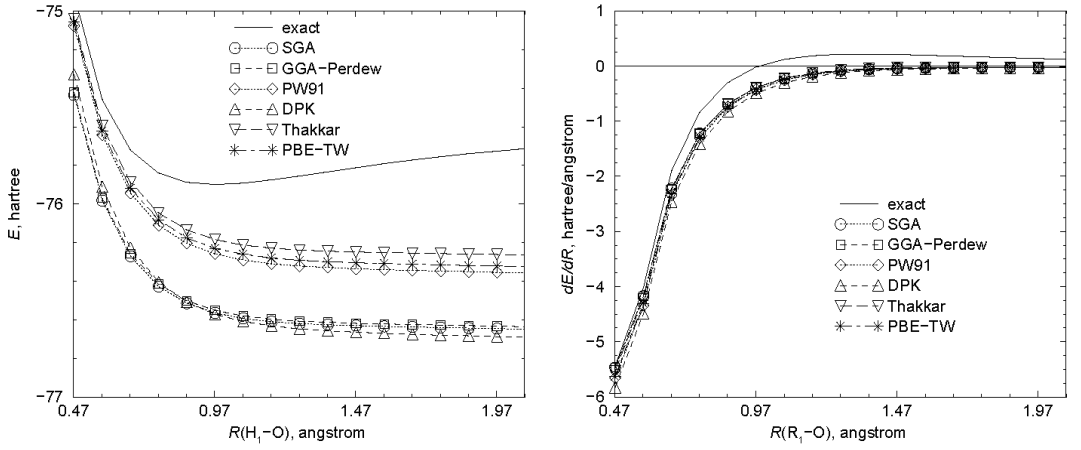

Figure 2. Total energy (left panel) and gradient of the total energy (right panel) of the H_2O molecule as a function of one bond length with the other fixed at the KS-LDA equilibrium distance (0.9714 Å), calculated using six approximate KE functionals and with KS-LDA densities (TZVP basis set) as input.

bond length for CO and H_2O (one bond stretched, the other clamped at the KS equilibrium value) respectively. Again, the OF-DFT total energy Eq. (6) was calculated from the converged KS density in the local density approximation. Calculations were done in a triple-zeta basis with polarization functions (TZVP) [29–31]) with T_s approximated by one of the selected functionals. None of the selected functionals correctly reproduces the behavior of the KS-LDA total energy near the equilibrium distance (R_e = 1.1318 Å for CO and $R(H_1–O)= R(H_2–O)= 0.9714$ Å for H_2O). In particular there is *no energy minimum*; none of the six functionals predicts a bound molecular state. The numerical errors increase in magnitude for $R \geq R_e$.

B. Interatomic forces

Because the approximate KE functionals fail to yield energy minima as a function of bond length, their predictions of interatomic forces at the LDA B-O level of approximation also are qualitatively incorrect. The B-O force on nucleus I is simply

$$\mathbf{F}_I = -\nabla_{\mathbf{R}_I} E^{\text{OF-DFT}}[n]\,. \tag{13}$$

Continuing with test computations which used the KS-LDA density as input, we show gradients of the OF-DFT total energy as a function of bond length for the CO and H_2O molecules, respectively, in the right-hand panels of Figs. 1 and 2. Consistent with the lack of energy minima just discussed, the force curves are purely repulsive, and what supposedly is the attractive region is described completely incorrectly. Clearly MD simulations cannot be based on any of these six approximate OF-DFT functionals.

We have not carried out the relatively laborious process of finding the density that minimizes the total energy with each of the six functionals studied. However, our work shows that these functionals cannot reproduce the KSLDA densities and simultaneously yield qualitatively correct B-O potential curves for representative small molecular systems.

C. The Pauli term

It has been very productive to employ known exact behaviors, (e.g. scaling, bounds, limits), as constraints on approximate forms for exchange-correlation functionals, as evidenced by the success of generalized gradient approximations (GGA) for E_{xc}. To extend that *constraint-based* framework to KE functionals, it is beneficial to use known properties, specifically to decompose the KS kinetic energy functional $T_s[n]$ into the von Weizsäcker term $T_W[n]$, plus a *non-negative* remainder, known as the Pauli term, $T_\theta[n]$ (see [32–35]):

$$T_s[n] = T_{\rm W}[n] + T_\theta[n]\,, \qquad T_\theta \geq 0\,. \tag{14}$$

The non-negativity of T_θ is a crucial advantage of this particular decomposition. Then the single Euler equation Eq. (7) corresponding to the electronic part of the OF-DFT energy $E^{\rm OF-DFT}$ functional takes the following Schrödinger-like form [33–35]:

$$\left\{-\frac{1}{2}\nabla^2 + v_\theta([n];\mathbf{r}) + v_{\rm KS}([n];\mathbf{r})\right\}\sqrt{n(\mathbf{r})} = \mu\sqrt{n(\mathbf{r})}\,, \tag{15}$$

where v_θ is the Pauli potential

$$v_\theta([n];\mathbf{r}) = \frac{\delta T_\theta[n]}{\delta n(\mathbf{r})}\,, \qquad v_\theta \geq 0\,. \tag{16}$$

Equation (15) follows from

$$v_{\rm W}([n];\mathbf{r}) \equiv \frac{\delta T_{\rm W}[n]}{\delta n(\mathbf{r})} = \frac{1}{\sqrt{n(\mathbf{r})}}(-\frac{1}{2}\nabla^2)\sqrt{n(\mathbf{r})}\,. \tag{17}$$

The exact formal expression for the Pauli KE kernel t_θ ($T_\theta = \int t_\theta d^3\mathbf{r}$) in terms of KS orbitals is defined [35] by

$$\begin{aligned} t_\theta([n];\mathbf{r}) &= t_{\rm orb}(\mathbf{r}) - \sqrt{n(\mathbf{r})}(-\frac{1}{2}\nabla^2)\sqrt{n(\mathbf{r})} \\ &= t_{\rm orb}(\mathbf{r}) - n(\mathbf{r})v_{\rm W}([n];\mathbf{r})\,. \end{aligned} \tag{18}$$

In Ref. [35] it is shown that t_θ is also *non-negative*: $t_\theta([n];\mathbf{r}) \geq 0$ for all $\mathbf{r}$, as one might expect.

A useful formal expression for v_θ in terms of t_θ and the KS orbitals and eigenvalues follows from an argument due to Levy and Ou-Yang [35], itself a variant on work of Bartolotti and Acharya [32]. Multiply Eq. (4) from the left by $\phi_i^*(\mathbf{r})$, sum over i, add $\varepsilon_{N'}$ to both sides, rearrange, and divide by $n(\mathbf{r})$. One gets:

$$\frac{t_{\rm orb}([n];\mathbf{r})}{n(\mathbf{r})} + \sum_{i=1}^{N'}(\varepsilon_{N'} - \varepsilon_i)\frac{|\phi_i(\mathbf{r})|^2}{n(\mathbf{r})} = \varepsilon_{N'} - v_{\rm KS}([n];\mathbf{r})\,. \tag{19}$$

Now, noting that from the exact asymptotic behavior of the electron density [1, 34, 35] we can identify μ of Eq. (7) as $\varepsilon_{N'}$, we use that equation to replace

the RHS of Eq. (19) with $\delta T_s[n]/\delta(\mathbf{r})$, which, based on Eq. (14) we write in the form $\delta T_s[n]/\delta(\mathbf{r}) \equiv v_{\mathrm{W}}([n];\,\mathbf{r})+v_\theta([n];\,\mathbf{r})$. Finally, replacing $t_{\mathrm{orb}}(\mathbf{r})$ by its equivalent as given in the second line of Eq. (18), we reach the exact result

$$v_\theta([n];\mathbf{r}) = \frac{t_\theta([n];\mathbf{r})}{n(\mathbf{r})} + \sum_{i=1}^{N'}(\varepsilon_{N'}-\varepsilon_i)\frac{|\phi_i(\mathbf{r})|^2}{n(\mathbf{r})}\,. \tag{20}$$

We reiterate that the non-negativity of v_θ,

$$v_\theta([n];\mathbf{r}) \geq 0\,, \tag{21}$$

is an extremely important property. It is explicit in Eq. (20), where v_θ is presented as a sum of two *non-negative* terms. As discussed above, the applications of OF-DFT we have in mind require that the orbital-dependent kinetic energy Eq. (3) be approximated. In view of Eqs. (14) and (18), finding an approximation for $T_s[\{\phi_i\}_{i=1}^{N'}]$ means finding an approximation for the Pauli term $T_\theta[n]$ such that these positivity constraints are respected.

Now consider the implications for interatomic force calculations of the introduction of approximations to T_s. From Eq. (13) and in notation that explicitly exhibits the roles of v_{W}, v_θ, and v_{KS}, the force assumes the form

$$\mathbf{F}_I = -\frac{\partial E_{\mathrm{ion}}}{\partial \mathbf{R}_I} - \int \left[v_{\mathrm{W}}([n];\mathbf{r}) + v_\theta([n];\mathbf{r}) + v_{\mathrm{KS}}([n];\mathbf{r})\right]\frac{\partial n(\mathbf{r})}{\partial \mathbf{R}_I}\,d^3\mathbf{r}\,. \tag{22}$$

Equation (22) shows that there are three sources of error for the calculated forces: errors introduced by approximation of the exchange-correlation energy (and the corresponding v_{KS}), those due to use of an approximate v_θ (obtained from an OF-KE functional), and those due to use of an approximate density n. Roughly speaking, an error in the calculated density will be of comparable effect in all three of the v terms in the integrand of Eq. (22). However, the approximated v_θ is much larger than the approximated part of v_{KS}, and errors in v_θ will dominate the force calculation unless the OF-KE functional is obtained to higher relative accuracy than the exchange-correlation functional.

D. Generalized gradient approximation and conjoint KE functionals

A gradient expansion for $T_s[n]$ which provides, at least in principle, a formal systematic way of improving upon the TF kinetic energy functional is given by (see [16–19] for details)

$$T_s[n] = \int \left\{ t_0([n];\mathbf{r}) + t_2([n];\mathbf{r}) + t_4([n];\mathbf{r}) + \ldots \right\} d^3\mathbf{r} \,. \tag{23}$$

Here $t_0 = t_{TF}$, t_2 is 1/9th of the Weizsäcker kinetic energy [Eq. (9)], and t_4 is

$$t_4([n];\mathbf{r}) = \frac{1}{540(3\pi^2)^{2/3}} n^{5/3}(\mathbf{r}) \left[\left(\frac{\nabla^2 n(\mathbf{r})}{n^{5/3}(\mathbf{r})} \right)^2 - \frac{9}{8} \left(\frac{\nabla n(\mathbf{r})}{n^{4/3}(\mathbf{r})} \right)^2 \left(\frac{\nabla^2 n(\mathbf{r})}{n^{5/3}(\mathbf{r})} \right) + \frac{1}{3} \left(\frac{\nabla n(\mathbf{r})}{n^{4/3}(\mathbf{r})} \right)^4 \right] . \tag{24}$$

The sixth-order term, which depends on n, $|\nabla n|$, $\nabla^2 n$, $|\nabla \nabla^2 n|$ and $\nabla^4 n$ was obtained in [17]. The Laplacian term $\nabla^2 n$ affects only the local behavior of the kinetic energy density since $\nabla^2 n$ integrates to zero, but there exist arguments both for including and for excluding it in the definition of the KE density functional; for example, see [19, 36].

Introducing the definition $k_F = (3\pi^2 n)^{1/3}$, we define the dimensionless *reduced density gradient*

$$s \equiv \frac{|\nabla n|}{(2k_F)n} = \frac{1}{2(3\pi^2)^{1/3}} \frac{|\nabla n|}{n^{4/3}} \tag{25}$$

(familiar in GGA XC approximations) and the *reduced density Laplacian*

$$p \equiv \frac{\nabla^2 n}{(2k_F)^2 n} = \frac{\nabla^2 n}{4(3\pi^2)^{2/3} n^{5/3}} \,. \tag{26}$$

Expressing the von Weizsäcker kinetic energy in terms of s, one finds $t_W = \frac{5}{3} s^2 t_0$, and using the partition of the KE functional defined by Eq. (14), the GEA of Eqs. (23)–(24) can be seen to correspond to the following expression for the Pauli KE:

$$T_\theta[n] = \int \left\{ t_\theta^{(0)}([n];\mathbf{r}) + t_\theta^{(2)}([n];\mathbf{r}) + t_\theta^{(4)}([n];\mathbf{r}) + \ldots \right\} d^3\mathbf{r} \,, \tag{27}$$

where

$$t_\theta^{(0)}([n];\mathbf{r}) = t_0([n];\mathbf{r}) \left[1 - \frac{5}{3} s^2 \right] , \tag{28}$$

$$t_\theta^{(2)}([n];\mathbf{r}) = t_0([n];\mathbf{r}) \left[\frac{5}{27} s^2 \right] , \tag{29}$$

and

$$t_\theta^{(4)}([n];\mathbf{r}) = t_0([n];\mathbf{r})\left[\frac{8}{81}\left(p^2 - \frac{9}{8}s^2 p + \frac{1}{3}s^4\right)\right]. \tag{30}$$

The SGA defined by Eqs. (28)–(29) improves significantly upon the Thomas-Fermi model; recall values in Table I. A related class of KE functionals has a form motivated by the generalized gradient approximation (GGA) for the exchange-correlation energy [20]. These KE functionals can be written

$$T_s^{\mathrm{GGA}}[n] = \int t_0([n];\mathbf{r}) F_{\mathrm{t}}(s(\mathbf{r}))d^3\mathbf{r}\,, \tag{31}$$

where F_{t} is a kinetic energy *enhancement factor* that is a functional of the reduced density gradient s. The SGA is a special case of the GGA form defined by the foregoing equation.

An equation parallel to Eq. (31) can be written to define the GGA form for the Pauli term (see [14]):

$$T_\theta^{GGA}[n] = \int t_0([n];\mathbf{r}) F_\theta(s(\mathbf{r}))d^3\mathbf{r}. \tag{32}$$

Here F_θ is a modified enhancement factor related to F_{t} by

$$F_\theta(s) = F_{\mathrm{t}}(s) - \frac{5}{3}s^2. \tag{33}$$

The *non-negativity* of t_θ means that F_θ also must be non-negative everywhere.

The consequences of these exact properties are illustrated in Fig. 3. For conventional KS calculations with LDA XC and using numerical orbitals, the figure shows the exact orbital-dependent t_θ, the corresponding Pauli potential v_θ and enhancement factor F_θ calculated along the internuclear axis for the N_2 and SiO diatomic molecules with slightly stretched bonds (see figure caption). The figure also shows the electronic density, scaled by an atomic-like radial factor to reveal the shell structure. All three quantities, t_θ, v_θ, and F_θ are everywhere *non-negative*, as they should be. A point that will become important shortly is that the exact v_θ is *finite* at the nuclei for both molecules and has local maxima in positions close to the inter-shell minima of the electronic density. The local maxima between the nuclei are lower than the

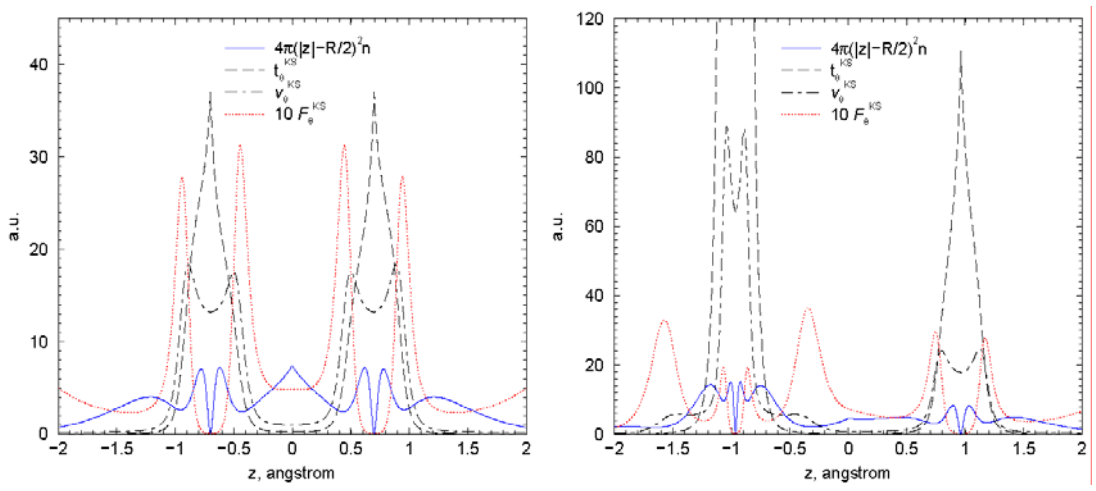

Figure 3. Electronic density (scaled by the factor $4\pi(|z| - R/2)^2$, with R the internuclear distance), Pauli term, Pauli potential, and enhancement factor F_θ [see Eq. (33)], calculated for points on the internuclear axis using KS LDA fully numerical orbitals. Left panel: N_2, atoms at (0, 0,±0.6993)Å; right panel: SiO, Si at (0, 0,−0.963), O at (0, 0,+0.963)Å.

maxima in the outer region to form a kind of confinement potential for the Schrödinger-like equation, Eq. (15). Analogous atomic results for the kinetic energy and modulating factor A_N (which is related to the enhancement factor F_t) are published in [37]. The relation between A_N and F_t is established in [38].

The GGA is highly successful in models for E_{xc}. Various authors therefore have sought to construct GGA kinetic energy functionals by exploiting the "conjoint gradient correction" hypothesis first put forward by Lee, Lee, and Parr (LLP) [25]. The LLP conjointness conjecture is that the KE enhancement factor $F_t(s)$ has the same analytical form as the enhancement factor $F_x(s)$ used in the GGA exchange energy functionals. This conjecture leads us to a more detailed consideration of enhancement factors.

We therefore examine the detailed form of the six KE functionals which were introduced in our initial tests, and also were studied as a representative set of semi-local explicit density functionals in Ref. [39]. The first of these functionals is:

(i) The SGA defined by $t_0 + t_2$, or

$$T_s^{\mathrm{SGA}}[n] = T_{\mathrm{TF}}[n] + \frac{1}{9}T_{\mathrm{W}}[n], \tag{34}$$

The other five functionals are defined by their enhancement factors F_t within the GGA form:

(ii) An *ab-initio* GGA functional proposed by Perdew [20] (GGA-P),

$$F_{\mathrm{t}}^{\mathrm{GGA\text{-}P}}(s(\mathbf{r})) = \frac{1 + 88.3960\, s^2(\mathbf{r}) + 16.3683\, s^4(\mathbf{r})}{1 + 88.2108\, s^2(\mathbf{r})}, \tag{35}$$

(iii) The PW91 kinetic energy functional constructed by Lacks and Gordon [21]. It is "conjoint" to the Perdew-Wang-91 exchange energy functional, and has the form

$$F_{\mathrm{t}}^{\mathrm{PW91}}(s(\mathbf{r})) = \frac{1 + 0.19645\, s(\mathbf{r})\ \mathrm{arcsinh}[7.7956\, s(\mathbf{r})] + \{0.2743 - 0.1508\, \exp[-100\, s^2(\mathbf{r})]\} s^2(\mathbf{r})}{1 + 0.19645\, s(\mathbf{r})\ \mathrm{arcsinh}[7.7956\, s(\mathbf{r})] + 0.004\, s^4(\mathbf{r})}. \tag{36}$$

(iv) The semi-empirical functional proposed by DePristo and Kress (DPK) [22], where $F_{\mathrm{t}}(s)$ is in the Padé approximant $P_{4,3}(s)$ form with some parameters fixed from the requirement of satisfaction of exact conditions on the KE and others determined by fitting to the known total kinetic energies of four closed shell atoms,

$$F_{\mathrm{t}}^{\mathrm{DPK}}(s(\mathbf{r})) = \frac{1 + 0.95\, y(\mathbf{r}) + 14.28111\, y^2(\mathbf{r}) - 19.57962\, y^3(\mathbf{r}) + 26.6477\, y^4(\mathbf{r})}{1 - 0.05\, y(\mathbf{r}) + 9.99802\, y^2(\mathbf{r}) + 2.96085\, y^3(\mathbf{r})}, \tag{37}$$

with $y(\mathbf{r}) = t_{\mathrm{W}}/9t_{\mathrm{TF}}$.

(v) A functional introduced by Thakkar [23] with the enhancement factor constructed as a heuristic combination of enhancement factors of different GGA functionals and with parameters fitted to the kinetic energies of 77 molecules (this functional is claimed to be one of the most accurate functionals of the GGA form),

$$F_{\mathrm{t}}^{\mathrm{Thakkar}}(s(\mathbf{r})) = 1 + \frac{0.0055\, [b\, s(\mathbf{r})]^2}{1 + 0.0253\, b\, s(\mathbf{r})\ \mathrm{arcsinh}[b\, s(\mathbf{r})]} - \frac{0.072\, b\, s(\mathbf{r})}{1 + 2^{5/3}\, b\, s(\mathbf{r})}, \tag{38}$$

with $b = 2(6\pi^2)^{1/3}$.

(vi) The Tran and Wesolowski functional [24] (PBE-TW), which includes an enhancement factor defined by a simple form first used for E_{x} by Becke [40] and later by Perdew, Burke, and Ernzerhof [41]:

$$F_{\mathrm{t}}^{\mathrm{PBE\text{-}TW}}(s) = 1 + \frac{C_1 s^2}{1 + a_1 s^2}, \tag{39}$$

with C_1 = 0.2319 and α_1 = 0.2748. The two parameters in the PBE-TW functional were adjusted to recover the exact KE of the He and Xe atoms. Because the enhancement factor is not precisely the same as in the underlying E_x approximation, the PBE-TW functional is not strictly conjoint, but close enough to be considered as such. It too is claimed to be among the most accurate GGA KE functionals.

As was mentioned in [39], the KE of finite molecular systems is almost totally determined by the behavior of F_θ over a relatively small range of reduced density gradient s, not the asymptotic regions. The various enhancement factors F_θ as functions of s^2 on the interval [0, 2] are shown in Fig. 4. Surprisingly, all six enhancement factors are indistinguishable on the scale of the figure for $s^2 < 1$ and have linear behavior close to those of the SGA: $F_\theta^{\mathrm{SGA}} = 1 - 1.4815\, s^2$. This behavior is important in analyzing what goes wrong with these six functionals.

For this purpose we look at the test molecule, N_2, whose accurate enhancement factor F_θ was shown in Fig. 3. The left panel of Fig. 5 shows gradients of the N_2 total energy as a function of internuclear distance. As in the earlier examples, none of the six tested functionals predicts a bound state, and what should be the attractive region of the gradient curve is qualitatively completely wrong. As discussed already, the dominant error in the calculated forces for such a non-self-consistent OF-DFT calculation (i.e., one with self-consistent conventional KS density as input) is introduced by the

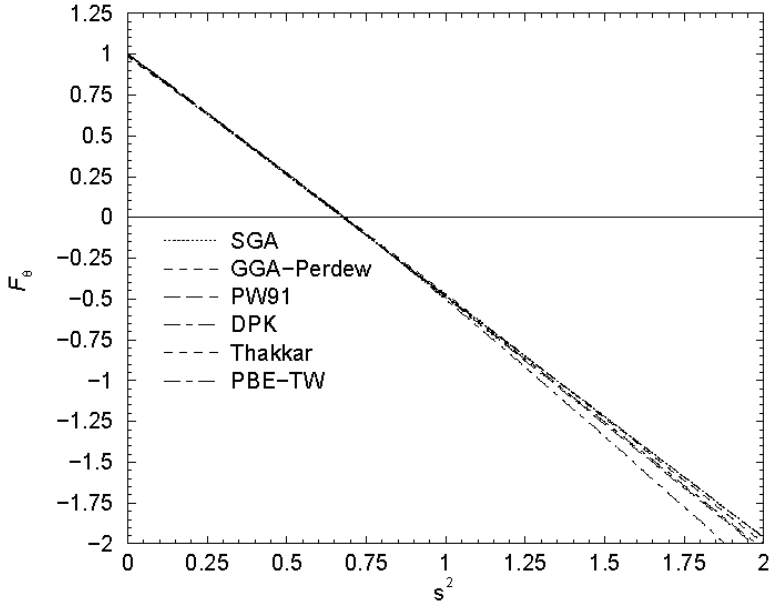

Figure 4. Enhancement factor F_θ of various GGA kinetic energy functionals as functions of s^2.

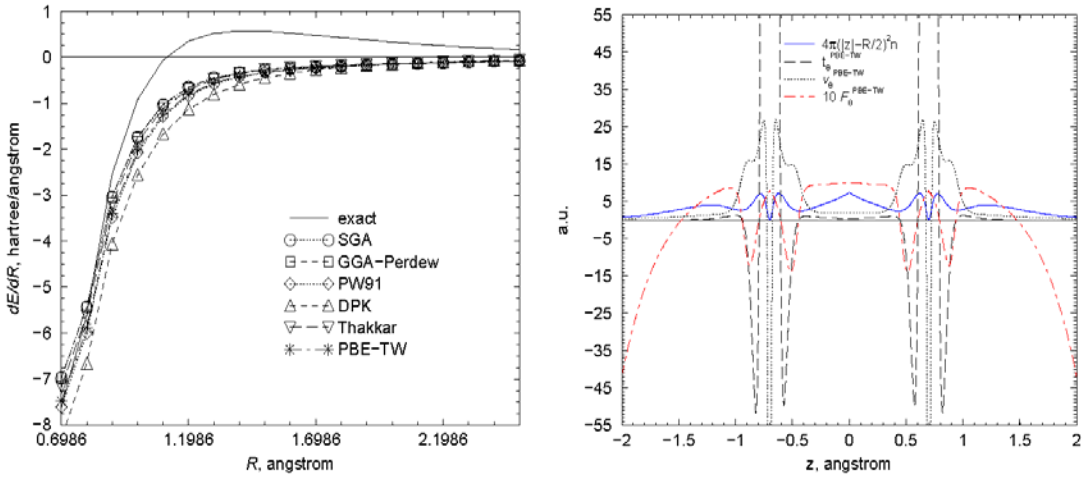

Figure 5. Left panel: Gradients of the total energy of the N_2 molecule for six KE functionals. Right panel, for N_2, atoms at (0, 0,±0.6993)Å: Electronic density (scaled by the factor $(4\pi(|z| - R/2)^2$, with R the internuclear distance), Pauli term, Pauli potential, and enhancement factor F_θ, calculated for points on the internuclear axis. The density is from a KS LDA calculation with fully numerical orbitals; the other data are from the conjoint GGA PBE-TW functional.

approximation for the Pauli term T_θ. We chose the PBE-TW functional for detailed tests; all six will give qualitatively the same outcomes. The right panel of Fig. 5 shows graphs of the approximate $t_\theta^{\mathrm{PBE-TW}}$, $v_\theta^{\mathrm{PBE-TW}}$ and $F_\theta^{\mathrm{PBE-TW}}$ for N_2, calculated along the internuclear axis for the same bond length within the attractive region as in Fig. 3. We see that the energy density of the Pauli term and corresponding enhancement factor have negative peaks in the inter-shell regions, a behavior that violates the condition of non-negativity of t_θ. Note, however, that we should remember the ambiguous definition of a kinetic energy density: adding $\nabla^2 n$ to the Pauli term will change only the local behavior of t_θ and F_θ, not the value of T_θ. The Pauli potential for the PBE-TW functional has very sharp negative peaks exactly at the nuclear positions, while the "exact" Pauli potential is finite at the nucleus and positive everywhere (compare to Fig. 3). The local inter-shell maxima are present, just as in the orbital-dependent KS results. Closer inspection of the figure shows, however, that the relative heights of these peaks do not correspond to those of the orbital-dependent KS results. The outer-region peaks are lower than the peaks lying in the inner internuclear space. In that sense, v_θ is not a confinement potential.

To understand the erroneous behavior of the GGA Pauli potential at the nuclei, let us analyze this term as was done in [39, 42]. Taking the functional derivative of the Pauli term, Eq. (32), we obtain

$$v_\theta^{\mathrm{GGA}}(\mathbf{r}) = \frac{5}{3}c_0 n^{2/3}(\mathbf{r})F_\theta(s(\mathbf{r})) + c_0 n^{5/3}(\mathbf{r})\frac{\partial F_\theta(s(\mathbf{r}))}{\partial s(\mathbf{r})}\left(\frac{\partial s(\mathbf{r})}{\partial n(\mathbf{r})} - \frac{5}{3}\frac{\nabla n(\mathbf{r})}{n(\mathbf{r})}\cdot\frac{\partial s(\mathbf{r})}{\partial \nabla n(\mathbf{r})} - \nabla\cdot\frac{\partial s(\mathbf{r})}{\partial \nabla n(\mathbf{r})}\right) - c_0 n^{5/3}(\mathbf{r})\frac{\partial^2 F_\theta(s(\mathbf{r}))}{\partial^2 s(\mathbf{r})}\nabla s(\mathbf{r})\cdot\frac{\partial s(\mathbf{r})}{\partial \nabla n(\mathbf{r})}. \tag{40}$$

Note that Eq. (34) of Ref. [39] omitted the last line of Eq. (40). In Ref. [39], we estimated the potential v_θ^{GGA} near a point nucleus from the nuclear-cusp behavior

$$n(\mathbf{r}) \sim \exp(-2Zr), \tag{41}$$

which follows from Kato's cusp condition [43] for an exact electron density (see also references in [3]):

$$\lim_{\mathbf{r}\to\mathbf{R}_I}\left\{\left(\frac{\partial}{\partial r} + 2Z_I\right)n_{av}(r)\right\} = 0\,. \tag{42}$$

Here n_{av} is the spherical average of the density and Z_I is the charge of nucleus I. If we take $F_\theta = 1 + as^2$ on the basis of the numerical evidence summarized in Fig. 4, after relatively simple algebra we find that

$$v_\theta^{GGA}(r) \sim \frac{a}{r}, \tag{43}$$

which shows that the GGA Pauli potential is singular at the nuclei. Moreover the singularity is negative, since $a < 0$ for the GGA functionals we tested (see Fig. 4). It follows that near the nuclei $v_\theta^{GGA} < 0$, which contradicts the requirement of non-negativity; recall Eq. (21). However, the improper negative sign of the singularity could be fixed by choosing an enhancement factor with a suitable Taylor series expansion near the nuclei; see subsequent discussion.

E. Modified conjoint kinetic energy functionals

As summarized in previous sections, all the tested KE functionals fail to provide qualitatively correct forces in what should be the attractive region for simple molecules (CO, H_2O, N_2). The situation is similar for many other diatomic and polyatomic molecules which we tested; most of these tests were on molecules containing Si–O bonds. We next consider how to make improvements without complicating the form of the enhancement factors.

The criterion for fitting the empirical parameters in many GGA-like KE functionals can be defined in terms of an *energetic* objective function, namely

$$\omega_E = \sum_{i=1}^{m} \left| E_i^{\mathrm{KS}} - E_i^{\mathrm{OF\text{-}DFT}} \right|^2 , \tag{44}$$

where ω_E is to be minimized over systems (atoms, molecules) indexed by i. When the parameter adjustment is done for fixed-density inputs (i.e., conventional KS densities as inputs), this total energy optimization is equivalent to optimization of the T_s functional.

In Ref. [39], to obtain a KE functional which is qualitatively correct in the attractive region for a single molecule, the authors tried to use the criterion Eq. (44) for different geometries of the SiO diatomic molecule. In that case the index i runs over different geometries of the system. The approach failed. In its place, a so-called ΔE criterion was used. The target function to be minimized is then

$$\omega_{\Delta E} = \sum_{M,i} \left| \Delta E_{M,i}^{\mathrm{KS}} - \Delta E_{M,i}^{\mathrm{OF\text{-}DFT}} \right|^2 , \tag{45}$$

where for nuclear configuration i of molecule M, $\Delta E_{M,i} = E_{M,i} - E_{M,e}$, with $E_{M,e}$ the energy associated with the equilibrium nuclear configuration as predicted from conventional KS computations. The criterion defined by Eq. (45) is almost equivalent to the direct fitting of a finite-difference approximation for the internuclear forces. Starting from enhancement factors with analytical forms equivalent to those for the exchange energy and using the ΔE criterion for parameter optimization, we obtained a set of modified conjoint KE functionals.

The most successful enhancement factors in that study were those defined by PBE-like analytical forms

$$F_t^{\mathrm{PBEn}}(s) = 1 + \sum_{i=1}^{n-1} C_i \left[\frac{s^2}{1 + a_1 s^2} \right]^i , \tag{46}$$

with $n = 2$ and $n = 4$. Parameters obtained by using the ΔE criterion for very specific small training sets (see details in [39]) are the following: $C_1 = 2.0309$ and $\alpha_1 = 0.2942$ for the PBE2 enhancement factor, and $C_1 = -7.2333$, $C_2 = 61.645$, $C_3 = -93.683$, and $\alpha_1 = 1.7107$ for PBE4. The modified conjoint PBE2 functional has exactly the same analytical form as the GGA-conjoint PBE-TW functional (but in the latter the parameters were chosen to recover the KE of the He and Xe atoms).

Figure 6 (left panel) compares PBE2 and KS ("exact") gradients of the total energy for N_2. The PBE-TW curve is plotted again for comparison. The

Pauli KE energy density t_θ, the Pauli potential v_θ, and the enhancement factor F_θ corresponding to the PBE2 functional are shown in the right panel. The main deficiency of the GGA KE functionals (the PBE-TW functional is taken as the example), namely the negative singularity of the Pauli potential at the nuclei, is eliminated in the modified conjoint PBE2 kinetic energy functional (compare with Fig. 5). The PBE2 Pauli potential is positive everywhere (see further comment below). As a result, the attractive region of the energy gradient surface is described at least qualitatively correctly (see right panel). Equations (40)–(43) also are valid for the modified conjoint KE functionals, and the PBE2 potential is still divergent at the nuclei in accordance with Eq. (43). The PBE2 Pauli energy density, t_θ and enhancement factor are positive in the inter-shell regions.

Though v_θ is properly positive everywhere, the observant reader may notice that this is not true for t_θ, which at large internuclear separations is in violation of the positivity constraint noted just after Eq. (18). However, the violation is inconsequential and does not cause a corresponding violation in v_θ, as other contributions to v_θ [cf. Eq. (20) for the exact v_θ] are positive and larger than the erroneous negative term. Moreover, v_θ is small within the

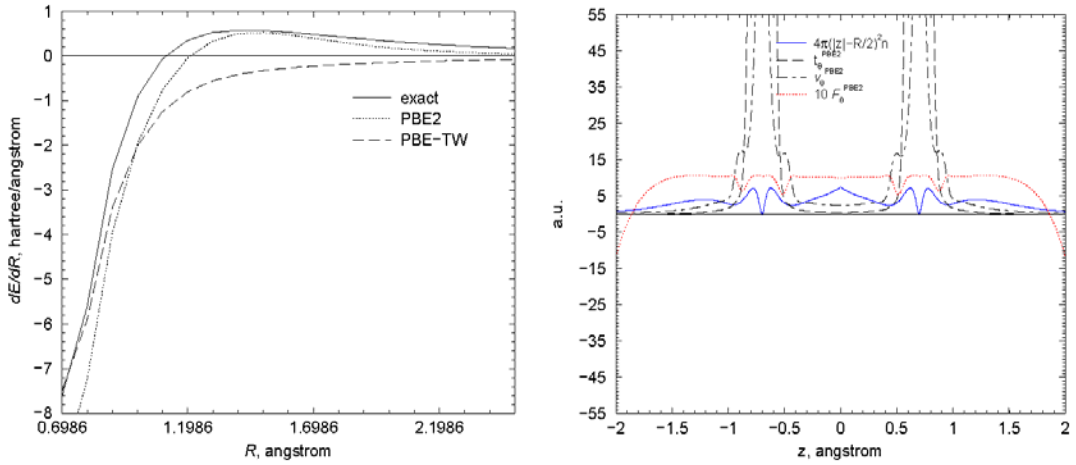

Figure 6. Left panel: Gradients of the total energy of the N_2 molecule for the PBE2 modified conjoint GGA potential, compared with results from the PBE-TW potential and the exact value. Right panel (in same layout as the right panel of Fig. 5), for N_2, atoms at (0, 0,±0.6993)Å: Electronic density (scaled by the factor $(4\pi(|z|-R/2)^2$, with R the internuclear distance), Pauli term, Pauli potential, and enhancement factor F_θ, calculated for points on the internuclear axis. The density is from a KS LDA calculation with fully numerical orbitals; the other data are from the PBE2 modified conjoint GGA functional.

region in question and in any case would not have a significant effect on the total energy.

Finally, we note that the exact Pauli potential Eq. (18) is finite at the nuclei (see Fig. 3). In contrast, the positive singularity of the PBE2 Pauli potential is an example of a remaining flaw that causes our modified conjoint functionals to overestimate the noninteracting kinetic energy T_s.

III. Reduced density derivatives approximation (RDA)

Equations (40)–(43) show that a divergence of the Pauli potential at the nuclei is an unavoidable property of any approximation for which the enhancement factor depends on the reduced density gradient only as, for example, in the GGA, GGA-conjoint and modified conjoint KE functionals. A resolution of this problem requires the finding of new variables for construction of KE enhancement factors. In Refs. [42] and [44], procedures involving such new variables were introduced. A preliminary summary of this new approach is presented here.

A. New variables: Reduced derivatives of the density

The gradient expansion in Eq. (27) can be rearranged straightforwardly into a GGA-like form:

$$t_\theta^{(2i)}([n];\mathbf{r}) = t_0([n];\mathbf{r})F_\theta^{(2i)}(s,p,...)\,, \tag{47}$$

where s, p, . . . are dimensionless density derivatives as defined in Section II; recall Eqs. (25) and (26). The first two terms of the expansion yield the SGA enhancement factor. From Eqs. (28) and (29), we have

$$F_\theta^{SGA} \equiv F_\theta^{(0)} + F_\theta^{(2)} = 1 + a_2 s^2\,, \tag{48}$$

with $\alpha_2 = -40/27$. The fourth-order term [cf. Eq. (30)] is F(4)

$$F_\theta^{(4)} = a_4 s^4 + b_2 p^2 + c_{21} s^2 p\,, \tag{49}$$

with coefficients $\alpha_4 = 8/243$, $b_2 = 8/81$, and $c_{21} = -1/9$.

With the foregoing functional forms as a guide, our objective is to identify combinations of the dimensionless derivatives (at this time only s and p) which lead to enhancement factors that are finite at the nuclei and

respect positivity. The first step is to evaluate the Pauli potential v_θ resulting from the forms in Eqs. (48) and (49), but with arbitrary values allowed for the coefficients appearing therein. Taking functional derivatives, and defining v_θ^{SGA}, $v_\theta^{(4)}$ to be the contributions to v_θ arising from the corresponding contributions to t_θ, we find after some manipulation

$$v_\theta^{\mathrm{SGA}} = c_0 n^{2/3}\left[\frac{5}{3} + a_2 s^2 - 2a_2 p\right], \tag{50}$$

$$v_\theta^{(4)} = c_0 n^{2/3}\left[\left(11a^4 + \frac{88}{9}c_{21}\right)s^4 - (5b_2 + 2c_{21})p^2 - \left(4a_4 - \frac{80}{9}b_2\right)s^2 p - \left(8a_4 + \frac{32}{3}c_{21}\right)q - \frac{20}{3}b_2 q' + 2b_2 q'' + 2c_{21}q'''\right], \tag{51}$$

where the new quantities q, q', q'', and q''' are dimensionless derivatives of order four:

$$q \equiv \frac{\nabla n \cdot (\nabla\nabla n)\cdot\nabla n}{(2k_F)^4 n^3} = \frac{\nabla n \cdot (\nabla\nabla n)\cdot\nabla n}{16(3\pi^2)^{4/3} n^{13/3}}, \tag{52}$$

$$q' \equiv \frac{\nabla n \cdot \nabla\nabla^2 n}{(2k_F)^4 n^2} = \frac{\nabla n \cdot \nabla\nabla^2 n}{16(3\pi^2)^{4/3} n^{10/3}}, \tag{53}$$

$$q'' \equiv \frac{\nabla^4 n}{(2k_F)^4 n} = \frac{\nabla^4 n}{16(3\pi^2)^{4/3} n^{7/3}}, \tag{54}$$

$$q''' \equiv \frac{\nabla\nabla n : \nabla\nabla n}{(2k_F)^4 n^2} = \frac{\nabla\nabla n : \nabla\nabla n}{16(3\pi^2)^{4/3} n^{10/3}}. \tag{55}$$

The operator denoted by a colon in the last two numerators corresponds to $A : B = \sum_{ij} A_{ij} B_{ji}$.

To find the behavior at the nuclei, we again invoke the form of the density at small distances r from a point nucleus of charge Z given in Eq. (41), with the result that the dimensionless derivatives s and q remain convergent and that

$$\lim_{r\to 0} s^2 = Z^2/[3\pi^2 n(0)]^{2/3}. \tag{56}$$

The remaining derivatives in Eqs. (50) and (51) have divergent limiting behaviors at small r. Substitution of the small-r limits of the dimensionless derivatives into Eqs. (50) and (51) gives

$$v_\theta^{\mathrm{SGA}}(r) \;=\; \frac{3a_2 Z}{5r} + \text{nonsingular terms}, \tag{57}$$

$$v_\theta^{(4)}(r) \;=\; \frac{c_0}{16[9\pi^4 n(r)]^{2/3}}\left[-\frac{16Z^2}{3r^2}\,(5b_2+3c_{21}) + \frac{32Z^3}{9r}\,(18a_4+17b_2+18c_{21})\right] + \text{nonsingular terms}. \tag{58}$$

Equation (57) confirms our earlier statement that an enhancement factor of the SGA form leads to a Pauli potential that is inherently singular (as $1/r$) at point nuclei. Clearly, without completely removing the s^2 term from F_θ^{SGA} we cannot choose its coefficient in a way that cures the singularity. However, the situation is quite different for the fourth-order contribution to the Pauli potential, $v_\theta^{(4)}$. The singularities in $v_\theta^{(4)}$ can be eliminated by the simple expedient of choosing α_4, b_2, and c_{21} so as to cause the r^{-2} and r^{-1} terms of Eq. (58) to have vanishing coefficients. That requirement leads to the relationships

$$\begin{aligned} c_{21} \;&=\; -\frac{5}{3}\,b_2\,, \\ a_4 \;&=\; \frac{13}{18}\,b_2\,, \end{aligned} \tag{59}$$

and leads us to define the *reduced derivative* of density (RDD) at fourth order to be

$$\kappa_4 = s^4 + \frac{18}{13}\,p^2 - \frac{30}{13}\,s^2 p\,. \tag{60}$$

A Pauli term defined by the enhancement factor of fourth order given in Eq. (49), but with parameters constrained by Eq. (59) (i.e. $F_\theta^{(4)}(\kappa_4) = a_4\kappa_4$), would produce a Pauli potential with *finite* values at the nuclei.

Though there is no direct means of removing the divergence of v_θ^{SGA} analogous to the way just shown for $v_\theta^{(4)}$, we can define, by analogy with Eq. (60), a second-order RDD:

$$\kappa_2 = s^2 + b_1 p\,. \tag{61}$$

Then we make the observation that

$$F_\theta^{(2)}(\kappa_2) = \frac{\kappa_2}{1+\alpha\kappa_2}\,, \tag{62}$$

produces, for small r, the Pauli potential

$$v_\theta^{(2)}(r) = C_1^{(2)}\frac{(1+C_2^{(2)}b_1\alpha)}{b_1\alpha^2} + O(r)\,, \tag{63}$$

where $C_i^{(2)} > 0$ are positive constants.

The strategy of requiring finiteness of an approximate Pauli potential at the nuclei may be used to define RDDs of mixed order in which different powers of s are combined. Observe that the Pauli potential for each $F_\theta(s) = s^n$ (n = 2, 4, ...) has the same type of singularity at small r, $v_\theta \sim 1/r$. Hence two divergent terms corresponding to different powers of s can be combined with coefficients that cause cancellation of the divergences. For example, the Pauli potential corresponding to the two-term enhancement factor $F_\theta^{(2,4)}(s) = a_2 s^2 + a_4 s^4$ is

$$v_\theta^{(2,4)}(r) = C_{24}\frac{(3\pi^{2/3}a_2 + 6^{1/3}a_4)}{r} + \text{nonsingular terms}, \tag{64}$$

and we can cause Eq. (64) not to have a nuclear-site divergence by taking $F_\theta^{(2,4)} = a_{24}\kappa_{24}$, where the reduced density derivative κ_{24} is defined as

$$\kappa_{24} \equiv s^2 - \frac{(3\pi)^{2/3}}{2^{1/3}}s^4\,. \tag{65}$$

Thus, we define a class of approximate KE functionals, the reduced derivative approximation (RDA) KE functionals, as those with enhancement factors written in terms of RDDs

$$T_s^{RDA}[n] \equiv T_{\rm W}[n] + \int t_0([n];\mathbf{r})F_\theta(\kappa_2(\mathbf{r}),\kappa_4(\mathbf{r}),\kappa_{24}(\mathbf{r}),..)\;d^3\mathbf{r}\,, \tag{66}$$

and having non-divergent Pauli potentials. This route of development of KE functionals is under active investigation. As already noted in the second-order case, not every enhancement factor or depending on κ_2, κ_4 etc. will produce a Pauli potential which is finite at the nuclei. Table II displays examples of analytical forms which produce finite and divergent Pauli potentials.

Table II. Examples of analytical forms of the F_θ enhancement factor that produce a Pauli potential with behavior at the nuclei that is finite ("Finite" column) or divergent ("Divergent" column). Here n,m = 1, 2, ...; $P_{n,m}(x)$ is the Padé approximant of order n,m; and κ_2, κ_4, and κ_{24} are reduced density derivatives defined in the text.

	Finite	Divergent
$F_\theta(\kappa_2)$	$\frac{1}{1+\alpha\kappa_2}$	κ_2^n
	$\left(\frac{\kappa_2}{1+\alpha\kappa_2}\right)^n$	$\frac{\kappa_2^{n+m}}{(1+\alpha\kappa_2)^n}$
	$\frac{\kappa_2^n}{(1+\alpha\kappa_2)^{n+1}}$	
	$P_{n,m}(\kappa_2),\ m=n \text{ or } n+1$	$P_{n,m}(\kappa_2),\ n \geq m+1$
$F_\theta(\kappa_4)$	κ_4	κ_4^{n+1}
	$\left(\frac{\kappa_4}{1+\alpha\kappa_4}\right)^n$	$\frac{\kappa_4^{n+m+1}}{(1+\alpha\kappa_4)^n}$
	$\frac{\kappa_4^{n+1}}{(1+\alpha\kappa_4)^n}$	
	$P_{n,m}(\kappa_4),\ n=m \text{ or } m+1$	$P_{n,m}(\kappa_4),\ n \geq m+2$
$F_\theta(\kappa_{24})$	κ_{24}^n	
	$\left(\frac{\kappa_{24}}{1+\alpha\kappa_{24}}\right)^n$	

B. Energy and forces simultaneously: Preliminary results

Reference [39] reported unsuccessful attempts to fit the parameters of a GGA form of KE functional for simultaneous prediction of energy and forces; recall brief mention above. Here we apply the *energy* criterion defined by Eq. (44) to the newly developed RDA functional form, comparing the results with our earlier studies in which modified conjoint functionals were fitted by the ΔE (optimized force) criterion.

The RDA functionals examined so far are of the simple two-parameter form

$$F_\theta^{\mathrm{RDA}(1,j)}(\kappa_4) = 1 + C\left(\frac{\kappa_4}{1+a\kappa_4}\right)^j; \tag{67}$$

the j values we considered were 2, 3, and 4. In this preliminary study we fitted the parameters C and a first to the KS interatomic potential for the

single molecule SiO, optimizing the parameters for a set of six bond lengths. We found it possible both to approach closely the KS data and to obtain qualitatively correct behavior in both the repulsive and attractive part of the potential curve. A second, separate set of parameters was also found to give a quantitatively satisfactory interatomic potential for N_2. The SiO data are presented in Fig. 7. The left panel of the figure shows that it is possible to obtain a potential curve of a qualitatively correct shape and energy from the RDA calculation, eliminating nearly all of the extremely large absolute energy error associated with the PBE2 calculation. Incidentally, we comment that this PBE2 energy error is larger than what we found to be typical. The right panel of the figure provides a comparison of the forces predicted by the various calculations. We see that both the approximate methods, PBE2 and RDA, predict the equilibrium bond length quite accurately, and that (as was pointed out in Section II-E) the PBE2 method yields very satisfactory interatomic forces in the entire attractive region and for the physically most important part of the repulsive region. The RDA curve, constructed with the more ambitious objective of reproducing both the absolute energy and the interatomic force, is qualitatively correct in both the attractive and repulsive regions, but with two to four times as much error as the PBE2 force curve.

We next attempted to study the transferability of the RDA parameters by optimizing a single parameter set (C, *a*) for the two molecules SiO and N_2. We were able to obtain potential curves that exhibited bonding for both molecules, albeit with energy errors that were three to four times as large as those found for the single-molecule fits.

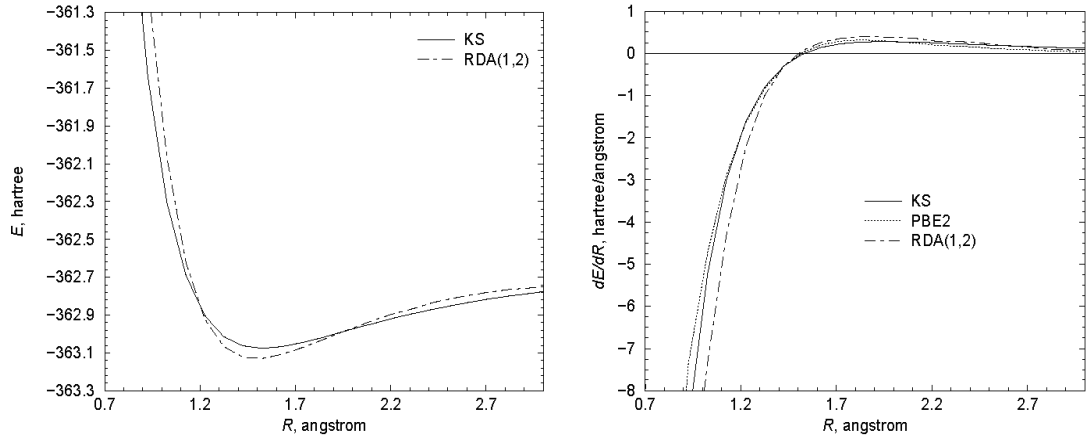

Figure 7. Total energy (left panel) and its derivative with internuclear distance (right panel) for SiO. Comparison of accurate Kohn-Sham (KS) results with those using the RDA kinetic-energy functional, Eq. (67), and the PBE2 modified conjoint kinetic-energy functional, Eq. (46). The PBE2 total energy is not visible in the left panel because it lies approximately 220 hartree higher than the other curves.

We close this section by observing that the methods used for singularity removal will only be effective if we ensure that the calculated densities satisfy Kato's cusp condition, and that the use of RDD's does not automatically guarantee the non-negativity of the Pauli potential. While the present study neither addresses these questions nor demonstrates full parameter transferability within the context of RDA calculations, the RDA approach appears quite promising.

IV. Non-self-consistent application to solids

Finally, we consider a very harsh test, namely the prediction of the equilibrium unit-cell volumes of two polymorphs of crystalline silica, namely coesite (48 atoms in unit cell, c/a = 1) and β-quartz (9 atoms in unit cell, c/a = 1.09). The objective was to compare the results from selected GGA KE functionals with those from a modified conjoint KE functional of the PBE4 functional form. The functionals were implemented in the SIESTA computational package [45] to provide tests similar to those reported for small molecules in Section II. Specifically, within SIESTA we used the PBE exchange-correlation functional, a norm-conserving NLPP [46] in the Troullier-Martins (TM) form [47], and a double zeta plus polarization (DZP) numerical atomic orbital (NAO) basis set. Unit-cell integrations were carried out by the Monkhorst-Pack scheme [48], with a $3\times2\times3$ point sampling for coesite and a $3\times3\times3$ grid for β-quartz. To simplify the calculations, the dependence of energy on cell volume was obtained by scaling the unit cell vectors without any attempt to optimize intra-cellular atomic positions.

The GGA KE functionals we studied for these crystalline systems were the SGA and that of Tran and Wesolowski (PBE-TW). The parameters of the PBE4 modified conjoint functional were obtained from a training set of three molecules with Si–O bonds by procedures discussed more fully in Ref. [39].

Our strategy was to determine how the calculated results are altered when we make precisely one change, namely to replace the conventional KS $T_s[\{\phi_i\}_{i=1}^{N'}]$ with the approximate $T_s[n]$, using the self-consistent density as input [42]. Strictly speaking, this is not the OF-DFT result for that approximate functional, because nonlocal pseudopotentials (NLPP) are used in the KS calculation, and there are small contributions to the total energy which depend on the orbitals through the pseudopotentials. We also note that the modified conjoint functionals were parameterized using all-electron densities, and there is no guarantee that these functionals will be fully appropriate for pseudopotentials and their pseudodensities. These limitations contribute to the severity of the test, making it provide an interesting comparison of the GGA and modified conjoint approximate KE functionals.

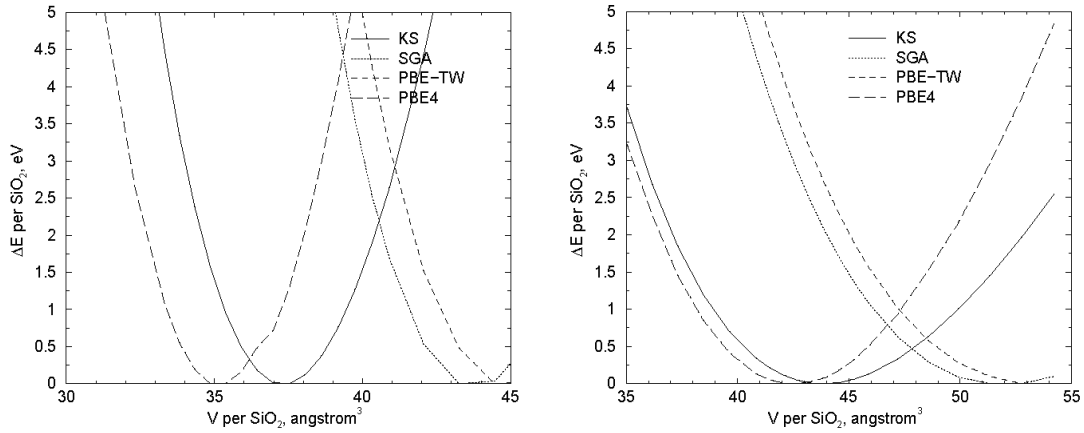

Figure 8. Total energy per SiO_2 unit, relative to equilibrium value, of coesite (left panel) and β-quartz (right panel), as a function of volume. Energies obtained using approximate KE functionals have been computed using KS densities.

Figure 8 shows the total energy per SiO_2 unit as a function of cell volume for each of the two silica polymorphs, calculated using the three OF-KE functionals (SGA, PBE-TW, and the modified conjoint functional PBE4), together with the results of the conventional (orbital-dependent) KS method. The most striking observation provided by the figure is that the PBE4 functional gives reasonable volumes per SiO_2 unit, correctly predicting the large specific volume difference between the two polymorphs. From a quantitative perspective the PBE4 results are also quite encouraging, yielding volumes only about 5% smaller than the "exact" values. In contrast, the GGA functionals overestimate the specific volumes by large amounts, with the more sophisticated PBE-TW giving poorer results than the relatively simpler SGA.

V. Discussion

The main ingredient needed for a successful OF-DFT approach is a reliable density functional for kinetic energy. While existing semi-local KE functionals of the GEA or GGA type predict reasonable values of the KE, they do not satisfactorily predict its change with geometric configuration and therefore do not yield acceptable interatomic forces, even for simple diatomic and polyatomic molecules. We have traced this poor performance to the violation of the non-negativity condition that must be satisfied by the Pauli potential, and have taken initial steps to remedy the situation by introducing modified conjoint KE functionals that correspond to acceptable Pauli potentials and generate qualitatively reasonable interatomic forces. The first modified conjoint functionals we have examined still have the deficiency that

they are singular at the nuclear positions; this does not make them qualitatively unacceptable, but does cause them to overestimate to some degree the kinetic energy. We have shown that it is not possible to develop purely GGA KE functionals that simultaneously satisfy positivity and finiteness of the Pauli potential.

We have carried out a preliminary investigation of the use of reduced density derivatives and related reduced-density-approximation functionals as a step toward the simultaneous description of kinetic energies and interatomic forces. At this point the functional forms we have examined, e.g. Eq. (67), may be too simple to be capable of providing robust and transferable KE functionals for practical OF-DFT applications. Work toward those objectives is underway. Note that Perdew and Constantin [49] recently have presented a KE functional involving a modified fourth-order gradient expansion and the decomposition of Eq. (14) (though they do not state it that way). We note that the form they propose involves a rather complicated functional interpolation between the gradient expansion and the von Weizsäcker functional. The paper does not discuss the corresponding potential v_θ and the performance for small molecule dissociation is characterized as "still not accurate enough for chemical applications". For us, these outcomes are additional confirmation of the opportunity for progress along the lines presented above.

Acknowledgments

We acknowledge informative conversations with Paul Ayers, Mel Levy, John Perdew, Eduardo V. Ludeña, and Yan Alexander Wang. This work was supported in part by the U.S. National Science Foundation, Grant DMR-0325553. We also acknowledge support from NSF Grants PHY-0601758 (FEH) and DMR-0218957 (SBT).

References

1. R.G. Parr and W. Yang, *Density Functional Theory of Atoms and Molecules* (Oxford, NY, 1989).
2. R.M. Dreizler and E.K.U. Gross, *Density Functional Theory* (Springer, Berlin, 1990).
3. E.S. Kryachko and E.V. Ludeña, *Energy Density Functional Theory of Many-Electron Systems* (Kluwer, Dordrecht, 1990).
4. W. Kohn and L. J. Sham, Phys. Rev. **140**, 1133 (1965).
5. P. Hohenberg and W. Kohn, Phys. Rev **136**, B864 (1964).
6. L. H. Thomas, Proc. Cambridge Phil. Soc. **23**, 542 (1927).
7. E. Fermi, Atti Accad. Nazl. Lincei **6**, 602 (1927).
8. E. Teller, Rev. Mod. Phys. **34**, 627 (1962).

9. Y.A. Wang and M.P. Teter, Phys. Rev. B **45**, 13196 (1992).
10. M. Foley and P.A. Madden, Phys. Rev. B **53**, 10589 (1996) and refs. therein.
11. Y.A. Wang and E.A. Carter, "Orbital-free Kinetic-energy Density Functional Theory", Chap. 5 in *Theoretical Methods in Condensed Phase Chemistry*, edited by S.D. Schwartz (Kluwer, NY, 2000) p. 117 and references therein.
12. N. Choly and E. Kaxiras, Sol. State. Commun. **121**, 281 (2002).
13. C. F. von Weizsäcker, Z. Phys. **96**, 431 (1935).
14. E.V. Ludeña and V.V. Karasiev. *Reviews of Modern Quantum Chemistry: a Celebration of the Contributions of Robert Parr*, edited by K. D. Sen (World Scientific, Singapore, 2002) p. 612.
15. J.P. Perdew, V. Sahni, M.K. Harbola, and R.K. Pathak, Phys. Rev. B **34**, 686 (1986).
16. C. H. Hodges, Can. J. Phys. **51**, 1428 (1973).
17. D.R. Murphy, Phys. Rev. A **24**, 1682 (1981).
18. W. Yang, Phys. Rev. A **34**, 4575 (1986).
19. W. Yang, R.G. Parr, and C. Lee, Phys. Rev. A **34**, 4586 (1986).
20. J.P. Perdew, Phys. Lett. A **165**, 79 (1992).
21. D.J. Lacks and R.G. Gordon, J. Chem. Phys. **100**, 4446 (1994).
22. A.E. DePristo and J.D. Kress, Phys. Rev. A **35**, 438 (1987).
23. A.J. Thakkar, Phys. Rev. A **46**, 6920 (1992).
24. F. Tran and T.A. Wesolowski, Int. J. Quantum Chem. **89**, 441 (2002).
25. H. Lee, C. Lee, and R.G. Parr, Phys. Rev. A **44**, 768 (1991).
26. G. L. Oliver and J. P. Perdew, Phys. Rev. A **20**, 397 (1979).
27. J.C. Slater, *The Self-Consistent Field for Molecules and Solids: Quantum Theory of Molecules and Solids* (McGraw-Hill, New York, 1974), vol. 4.
28. S.H. Vosko, L. Wilk, and M. Nusair, Can. J. Phys. **58**, 1200 (1980).
29. A. Schäfer, H. Horn, and R. Ahlrichs, J. Chem. Phys. **97**, 2571 (1992).
30. A. Schäfer, C. Huber, and R. Ahlrichs, J. Chem. Phys. **100**, 5829 (1994).
31. Taken from the Extensible Computational Chemistry Environment Basis Set Database, Version 02/25/04, Molecular Science Computing Facility, Environmental and Molecular Sciences Laboratory, Pacific Northwest Laboratory, P.O. Box 999, Richland, Washington 99352, USA, funded by the U.S. Department of Energy (contract DE-AC06-76RLO). See http://www.emsl.pnl.gov/forms/basisform.html
32. L.J. Bartolotti and P.K. Acharya, J. Chem. Phys. **77**, 4576 (1982).
33. B.M. Deb and S.K. Ghosh, Int. J. Quantum Chem. **23**, 1 (1983).
34. M. Levy, J.P. Perdew, and V. Sahni, Phys. Rev. A **30**, 2745 (1984), and references therein.
35. M. Levy, and H. Ou-Yang, Phys. Rev. A **38**, 625 (1988).
36. P.W. Ayers, R.G. Parr, and A. Nagy, Int. J. Quantum Chem. **90**, 309 (2001).
37. V.V. Karasiev, E.V. Ludeña, and A.N. Artemyev, Phys. Rev. A **62**, 062510 (2000).
38. R. Pis Diez and V. Karasiev, J. Phys. B **36**, 2881 (2003).
39. V.V. Karasiev, S.B. Trickey, and F.E. Harris, J. Comp.-Aided Mat. Des. **13**, 111 (2006).

40. A.D. Becke, J. Chem. Phys. **84**, 4524 (1986).
41. J.P. Perdew, K. Burke, and M. Ernzerhof, Phys. Rev. Lett. **77**, 3865 (1996).
42. V.V. Karasiev, R.S. Jones, S.B. Trickey, and F.E. Harris, "Constraint-based Single-point Kinetic Energy Density Functionals", Phys. Rev. B (submitted).
43. T. Kato, Commun. Pure Appl. Math. **10**, 151 (1957).
44. V.V. Karasiev, R.S. Jones, S.B. Trickey, and F.E. Harris. *12th International Conference on the Applications of Density Functional Theory in Physics and Chemistry*, Abstractbook, p. 184 (2007).
45. Spanish Initiative for Electronic Simulations with Thousands of Atoms (SIESTA); Version 2.0.; http://www.uam.es/departamentos/ciencias/fismateriac/siesta/. See also J. M. Soler, E. Artacho, J. D. Gale, A. García, J. Junquera, P. Ordejón, and D. Sánchez-Portal, J. Phys.: Condens. Matter **14**, 2745 (2002).
46. W.C. Topp and J.J. Hopfield, Phys. Rev. B **7**, 1295 (1973).
47. N. Troullier and J.L. Martins, Phys. Rev. B **43**, 1993 (1991).
48. H.J. Monkhorst and J.D. Pack, Phys. Rev. B **13**, 5188 (1976).
49. J.P. Perdew and L.A. Constantin, Phys. Rev. B **75**, 1155109 (2007).